

# High- $p_T$ experimental results on QCD

Javier Llorente  
on behalf of the ATLAS and CMS Collaborations.

Simon Fraser University

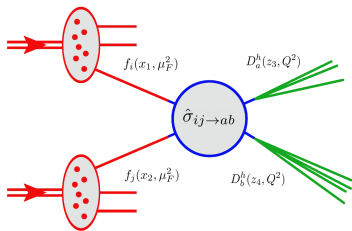
LHCP 2022 - May 20, 2022



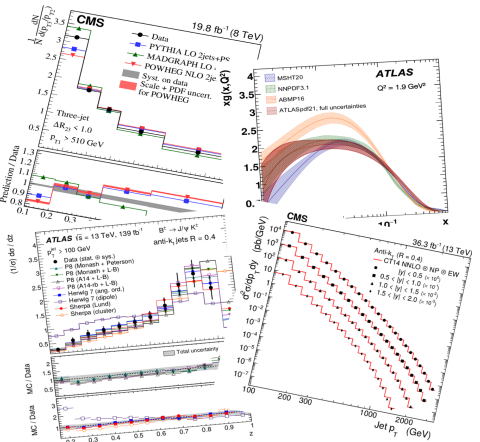
# Introduction

- The QCD cross section can be factorised in three parts: IS, HS, FS.
- ATLAS and CMS have presented important QCD results recently.
- Measurements are exploited to understand these three parts separately.

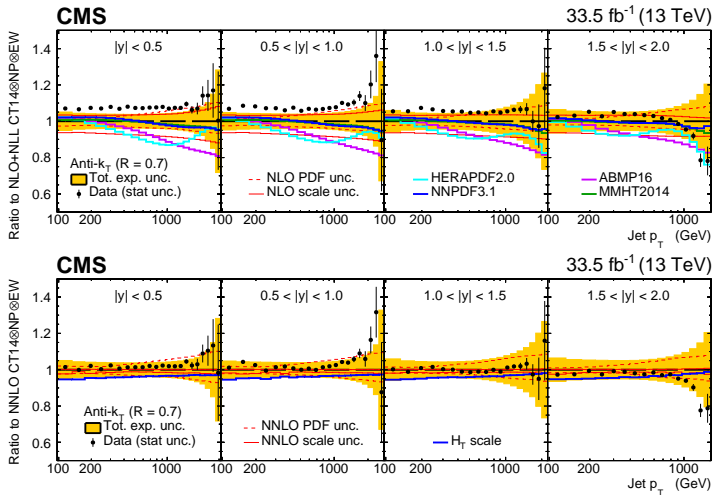
- Initial State  $\Rightarrow$  Parton Density  $f_i(x, \mu_F)$
- Hard Scattering  $\Rightarrow$  Matrix Element  $\hat{\sigma} \propto |\mathcal{M}|^2$
- Final State  $\Rightarrow$  Fragm. Functions  $D_a^h(z, \mu_f)$



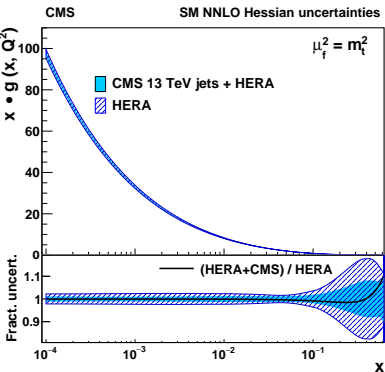
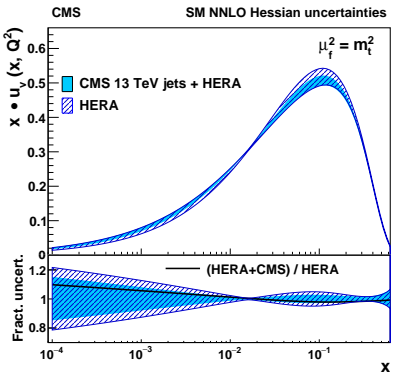
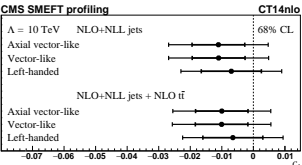
$$d\sigma = \sum_{i,j,a,b} \int_{\Omega} d^2\vec{x} d^2\vec{z} f_i(x_1, \mu_F^2) f_j(x_2, \mu_F^2) \times d\hat{\sigma}_{ij \rightarrow ab}(\vec{x}, \mu_R^2) \times D_a^h(z_3, \mu_f^2) D_b^h(z_4, \mu_f^2)$$



- Differential cross section as a function of  $(p_T, y)$  for  $R = 0.4$  and  $R = 0.7$ .
- Comparison to NLO+NLL and NNLO pQCD  $\otimes$  NP and EW effects.
- Description is well improved at NNLO with respect to NLO.



- Full QCD analysis includes HERA DIS and CMS  $t\bar{t}$  data.
  - PDFs as  $xf(x) = A_f x^{B_f} (1-x)^{C_f} (1 + D_f x + E_f x^2)$ .
  - Improved uncertainties on PDF by including jet data.
  - Wilson coefficient for 4-quark CI obtained for different  $\Lambda$ .
  - Limits on CI are set to  $\Lambda > 24$  TeV @ 95% CL.

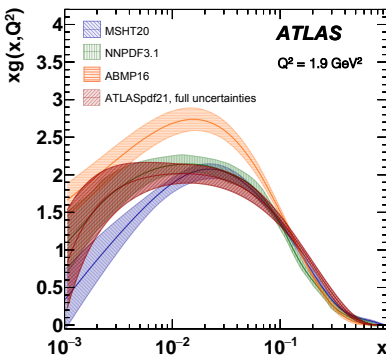
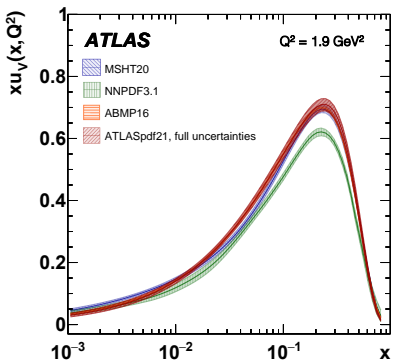
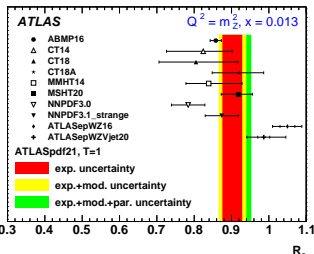


$$\alpha_s(m_Z) = 0.1170 \pm 0.0014 \text{ (fit)} \pm 0.0007 \text{ (model)} \pm 0.0008 \text{ (scale)} \pm 0.0001 \text{ (param.)}$$

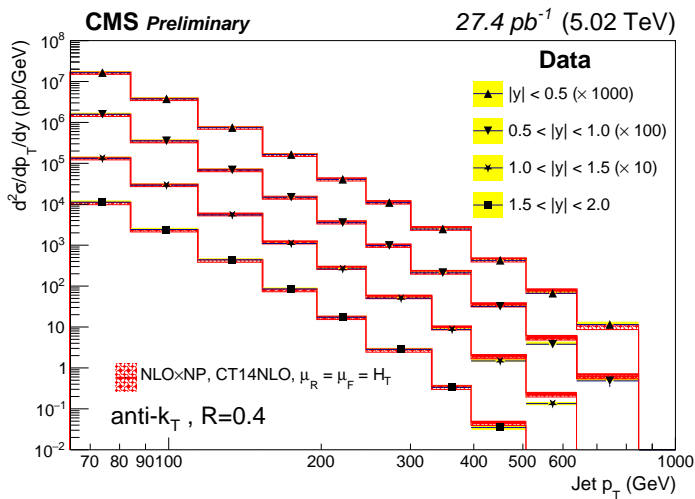
- Determination of PDFs from HERA + ATLAS data at different  $\sqrt{s}$ .
- PDF parameterisation follows the generic formulation:
  - Quarks:  $xq_i(x) = A_i x^{B_i} (1-x)^{C_i} P_i(x)$
  - Gluons:  $xg(x) = A_g x^{B_g} (1-x)^{C_g} P_g(x) - A'_g x^{B'_g} (1-x)^{C'_g}$
- For all PDFs  $P_i(x) = 1 + D_i x + E_i x^2 + F_i x^3$ .
- $D, E, F$  are non-zero only if  $\chi^2$  decreases significantly  $\Rightarrow$  21 parameters in total.
- $\chi^2$  fit includes full correlation between uncertainties.

Data set	$\sqrt{s}$ [TeV]	Luminosity [ $\text{fb}^{-1}$ ]	Decay channel	Observables entering the fit
Inclusive $W, Z/\gamma^*$	7	4.6	$e, \mu$ combined	$\eta_\ell (W), y_Z (Z)$
Inclusive $Z/\gamma^*$	8	20.2	$e, \mu$ combined	$\cos \theta^*$ in bins of $y_{\ell\ell}, m_{\ell\ell}$
Inclusive $W$	8	20.2	$\mu$	$\eta_\mu$
$W^\pm + \text{jets}$	8	20.2	$e$	$p_T^W$
$Z + \text{jets}$	8	20.2	$e$	$p_T^{\text{jet}}$ in bins of $ y^{\text{jet}} $
$t\bar{t}$	8	20.2	lepton + jets, dilepton	$m_{t\bar{t}}, p_T^t, y_{t\bar{t}}$
$t\bar{t}$	13	36		$m_{t\bar{t}}, p_T^t, y_t, y_{t\bar{t}}^b$
Inclusive isolated $\gamma$	8, 13	20.2, 3.2	-	$E_T^\gamma$ in bins of $\eta^\gamma$
Inclusive jets	7, 8, 13	4.5, 20.2, 3.2	-	$p_T^{\text{jet}}$ in bins of $ y^{\text{jet}} $

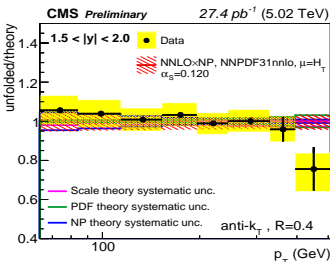
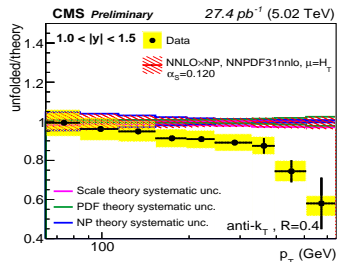
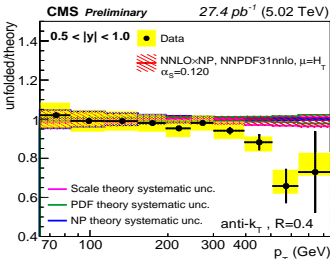
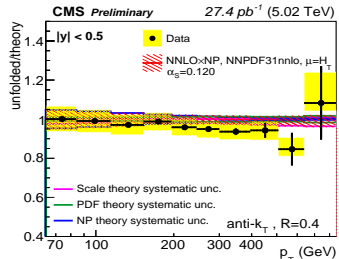
- Inclusion of ATLAS data brings ATLAS PDF close MSHT20 than HERAPDF.
- Comparison to CT18, NNPDF, MSHT20, ...
- Measurement of  $R_s(x, Q^2) = x(s + \bar{s})/x(\bar{u} + \bar{d})$ .
- Uncertainties estimated using different tolerances  $\chi^2 = T^2$ ;  $T = 1, 3$ .



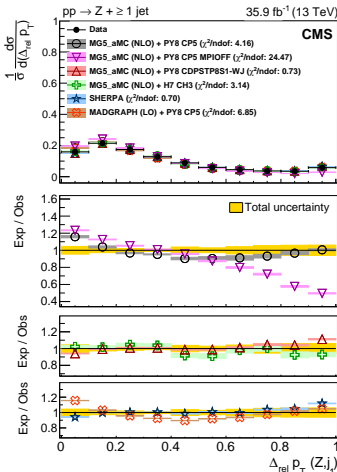
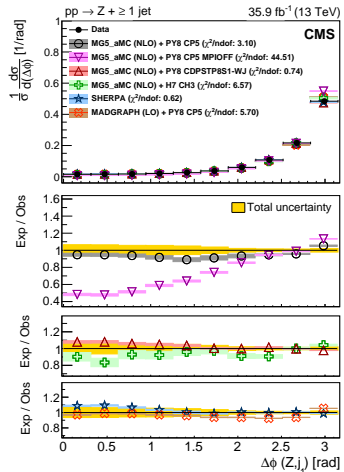
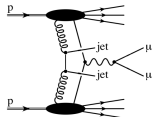
- Double-differential inclusive jet cross section as a function of  $(p_T, y)$ .
- Comparison to theoretical pQCD predictions at NLO and NNLO.



- NNLO scale uncertainties reduced with respect to NLO.  $\mu_R = \mu_F = \hat{H}_T$ .
- Best agreement is observed for NNPDF31 with  $\alpha_s(m_Z) = 0.120$ .

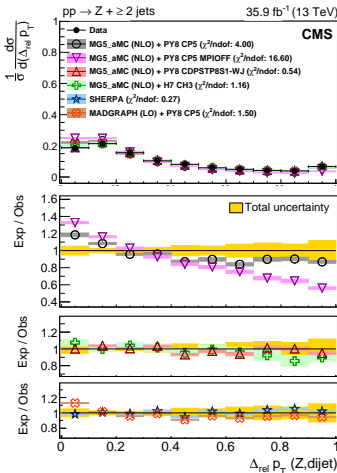
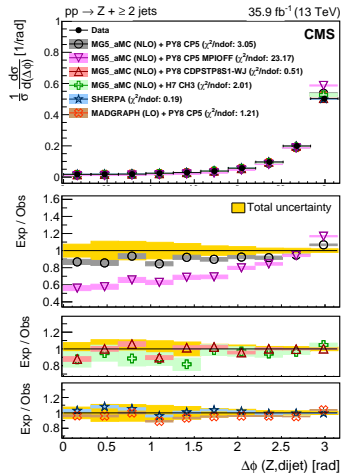


- Measurement of  $Z + \geq 1$  jet and  $Z + \geq 2$  jets in  $\mu\mu$  channel.
- Azimuthal separation  $\Delta\phi(Z, j_1)$  and  $\Delta\phi(Z, \text{dijet})$ .
- $p_T$ -balance  $\Delta_{\text{rel}} p_T(Z, j_1) = \frac{|\vec{p}_T(Z) + \vec{p}_T(j_1)|}{|\vec{p}_T(Z)| + |\vec{p}_T(j_1)|}$  and  $\Delta_{\text{rel}} p_T(Z, \text{dijet})$ .

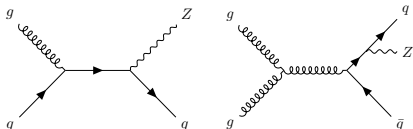


# CMS Z+jets sensitivity to DPS at $\sqrt{s} = 13$ TeV [JHEP 10, 176 (2021)]

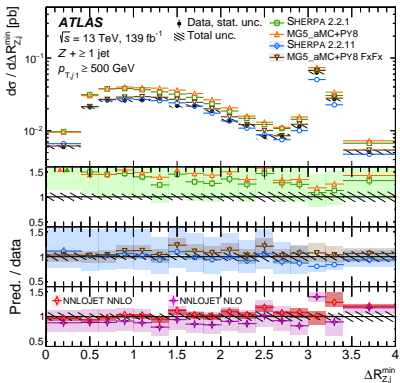
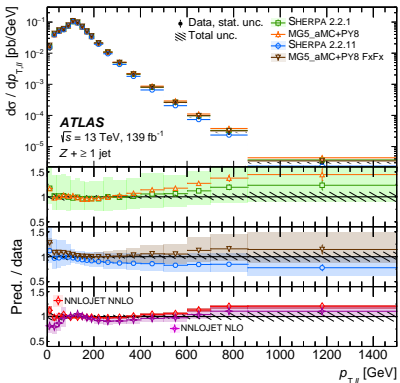
- Measurements are compared to different predictions at different orders.
- MG5\_aMC with different MPI and fragmentation tunes (and without MPI!).
- Sherpa merged NLO samples with up to 2 partons in final state.
- The effect of DPS is clearly seen when setting MPI off.



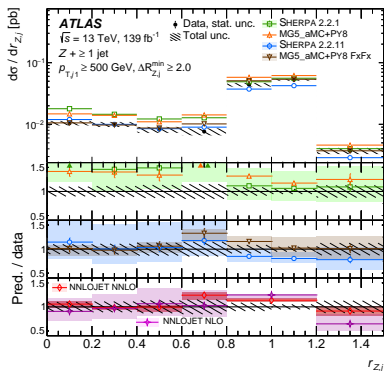
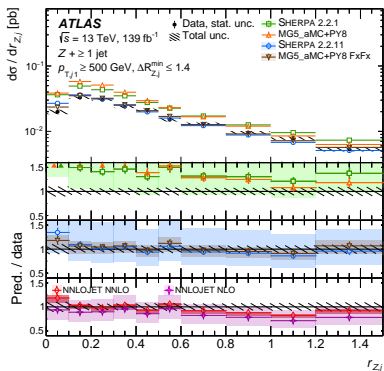
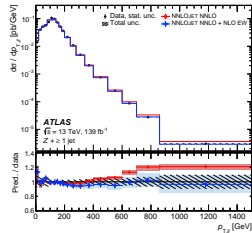
- $Z \rightarrow ee$  ( $\mu\mu$ ) with additional jets ( $p_T > 100$  GeV).
- High- $p_T$  region is selected with  $p_T^{\text{jet}} > 500$  GeV.
- $Z$ -boson radiation  $\propto \alpha_s \ln^2(p_{T,j_1}/m_Z)$ .



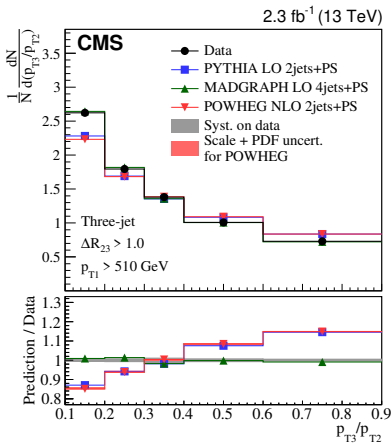
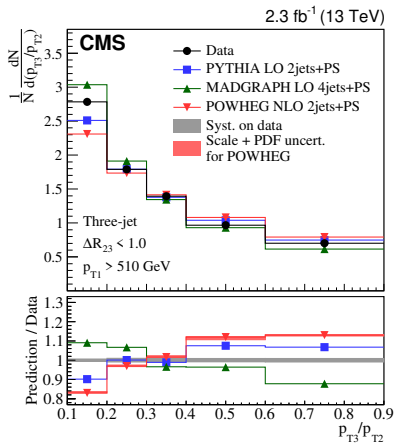
- Characterized in different topologies (collinear, back-to-back) using  $\Delta R_{Zj}$ .
- Comparison to different ME+PS and fixed-order predictions.



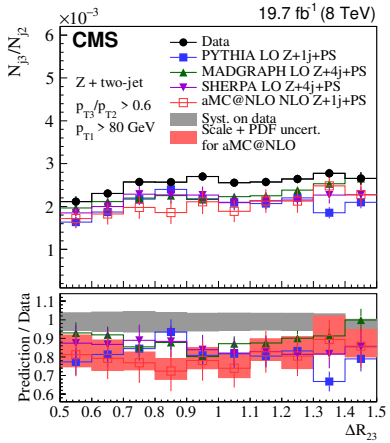
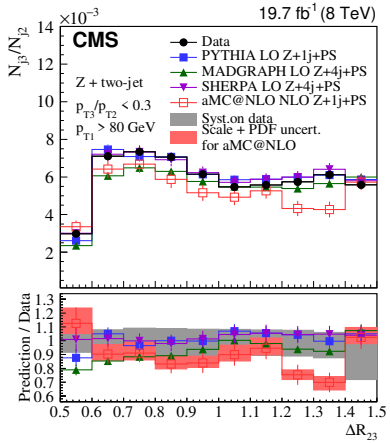
- Measurement of  $r_{Zj} = \frac{p_T^{\ell\ell}}{p_T(\text{closest jet})}$  in  $\Delta R$  bins.
- Excellent description by NNLO QCD + NLO EW.
- Sherpa 2.2.1 and MG5\_aMC+Py8 overestimate the cross section at high  $p_T$ .
- Sherpa 2.2.11 and FxFx merging for MG5\_aMC+Py8 provide an improved description.



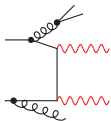
- Collinear/large-angle and soft/hard radiation in different final states.
- Measurement of  $\Delta R_{23}$  and  $p_{T3}/p_{T2}$  in three-jet and  $Z+2$ -jet events.
- $Z+2$ -jet measurement at  $\sqrt{s} = 8$  TeV, 3-jets at  $\sqrt{s} = 8$  and 13 TeV.
- Multi-let MG5\_aMC describes better the wide-angle region.



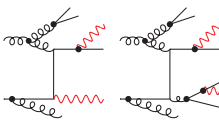
- Measurement of  $\Delta R_{23}$  for soft and hard emissions.
- In general, ME+PS describe the data better for soft regions.
- Hard-emission regions underestimated by theoretical predictions.



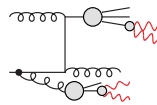
- Measurement of  $\gamma\gamma$  production for  $p_T(\gamma_1) > 40$  GeV,  $p_T(\gamma_2) > 30$  GeV.
- Background estimated from (ID, iso) sidebands for 2 photons (16 regions).
- Signal includes direct and fragmented  $\gamma$ , against non-prompt background.
- Poisson likelihood fit performed separately on each bin of each observable.



Direct photons



Fragmented photons

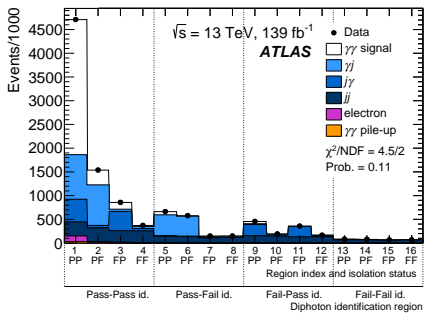


Non-prompt photons

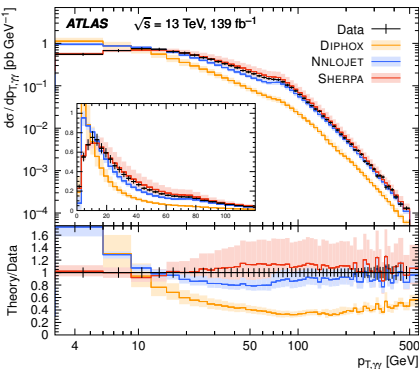
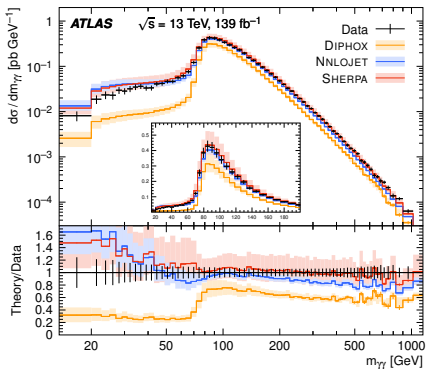
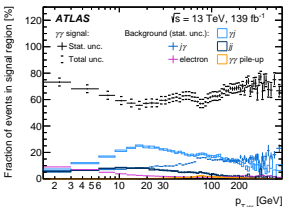
		Leading candidate isolation			
		Pass	Fail	Pass	Fail
Sub-leading candidate identification	Fail	6	8	14	16
	Pass	5	7	13	15
	Fail	2	4	10	12
	Pass	1	3	9	11

Signal region

Leading candidate identification



- Comparison to ME+PS and fixed-order pQCD predictions.
- Sherpa (NLO) and NNLOJet give a good description.
- NNLOJet provides improved scale precision wrt NLO.
- DiPhox (NLO) fails to describe the data.

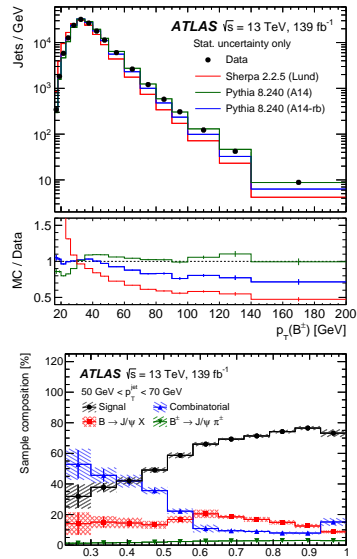
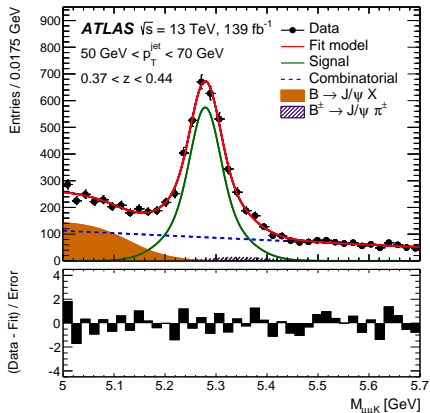


# ATLAS $b$ -fragmentation to $B^\pm$ at $\sqrt{s} = 13$ TeV [JHEP 12, 131 (2021)]

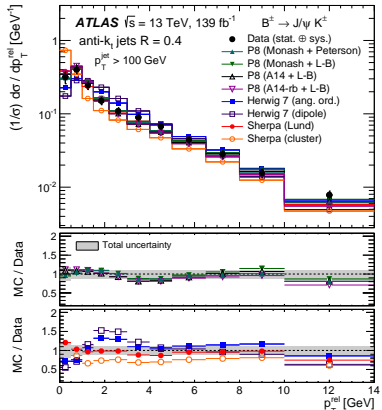
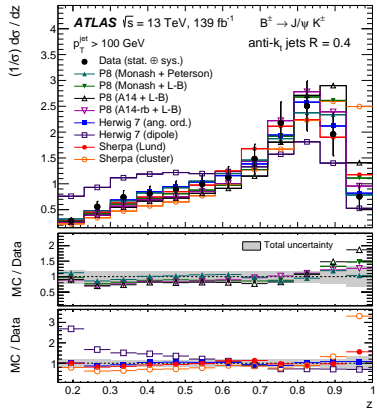
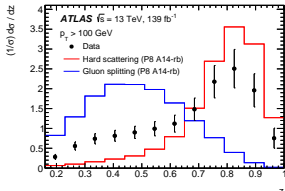
- Fragmentation observables for jets containing  $B^\pm \rightarrow J/\psi K^\pm$  at  $\Delta R < 0.4$
- Fully reconstructed decay from  $\mu\mu K$  tracks.
- Longitudinal and transverse profiles of  $B^\pm$ :

$$z = \frac{\vec{p}_J \cdot \vec{p}_B}{|\vec{p}_J|^2}; \quad p_T^{\text{rel}} = \frac{|\vec{p}_J \times \vec{p}_B|}{|\vec{p}_J|}$$

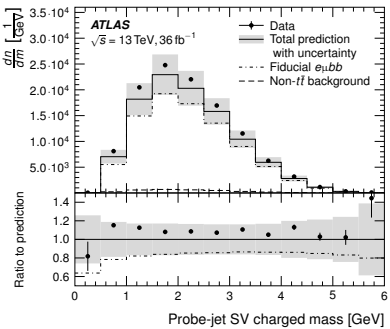
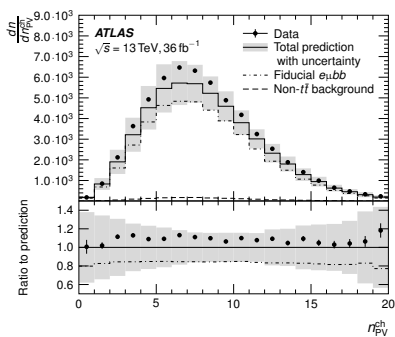
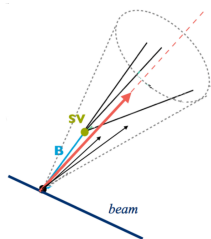
- Background estimated using  $M_{\mu\mu K}$  likelihood fits.



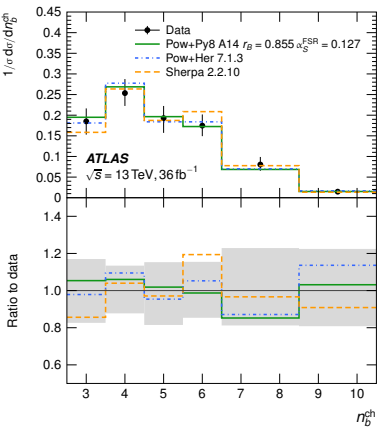
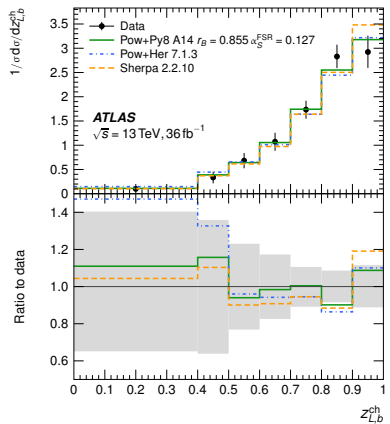
- Comparison to different ME+PS+fragmentation models.
- Pythia, Sherpa, H7 with different fragmentation/PS.
- Sensitivity to  $g \rightarrow b\bar{b}$  splitting is investigated.
- Discrepancies observed with H7 dipole shower ( $g \rightarrow b\bar{b}$ ).
- Sherpa cluster model shows discrepancies at high  $z$ .



- Event selection in  $t\bar{t} \rightarrow b\bar{b}e^\pm\mu^\mp$  dileptonic events.
- Exactly two jets: tag one jet, use the other as probe.
  - Probe jet should contain SV with at least 3 tracks.
  - If both jets are tagged, both jets are measured.
- Tracks from secondary vertex used to reconstruct  $\vec{p}_b^{ch}$ .
- All ghost-associated tracks used to reconstruct  $\vec{p}_{jet}^{ch}$ .



- Results are in reasonable agreement with MC expectations.
- Powheg + Pythia 8 gives a good description of the data.
- Powheg + Herwig 7.1.3 shows large differences at low  $z$ .
- Sherpa 2.2.10 provides the best overall description.



- Interesting dependence with  $\alpha_s^{\text{FSR}}$ . No dependence with  $\alpha_s^{\text{ISR}}$ .

## Summary and conclusions

- Wide variety of QCD measurements recently released at the LHC.
- Different analyses sensitive to different aspects of the QCD modelling.
- PDF fits have been performed by ATLAS and CMS.
- Inclusive jet cross sections at different values of  $\sqrt{s}$ .
- $Z+jets$  and multijet final states are thoroughly explored.
  - $Z+jets$  measurement in different topologies.
  - Three-jet events in different angular and momentum phase spaces.
- Diphoton cross section compared to theoretical predictions up to NNLO.
- $b$ -quark fragmentation explored by ATLAS in two different final states.
  - In dijets with  $B^\pm$  production, with explicit sensitivity to  $g \rightarrow b\bar{b}$ .
  - In  $t\bar{t}$  using charged momentum of  $B$ -hadrons.
- Stay tuned for more interesting results!